

*Carnegie Observatories Astrophysics Series, Vol. 3:
Clusters of Galaxies: Probes of Cosmological Structure and Galaxy Evolution
ed. J. S. Mulchaey, A. Dressler, and A. Oemler (Cambridge: Cambridge Univ. Press)*

Using the Sunyaev-Zel'dovich Effect to Probe the Gas in Clusters

MARK BIRKINSHAW

Department of Physics, University of Bristol

Abstract

The thermal Sunyaev-Zel'dovich effect is an important probe of clusters of galaxies, and has the attractive property of being proportional to the thermal energy content of the intracluster medium. With the assistance of X-ray data, the effect can be used to measure the number of hot electrons in clusters, and thus measure cluster baryon contents. Cluster absolute distances and other structural parameters can also be measured by combining thermal Sunyaev-Zel'dovich, X-ray, and other data. This review presents an introduction to the effect, shows some representative results, and sketches imminent developments.

1.1 Introduction

Ever since the cosmic microwave background radiation was discovered and interpreted as a thermal signal coming from the epoch of decoupling (Dicke et al. 1965; Penzias & Wilson 1965), it has been seen as a major cosmological tool. High-quality information about the background radiation is now available. The *COBE* mission demonstrated that the spectrum of the microwave background radiation is precisely thermal, with a temperature $T_{\text{rad}} = 2.728 \pm 0.002$ K (where necessary, all errors have been converted to $\pm 1\sigma$), and a maximum distortion characterized by a Comptonization parameter (§ 1.2.1) $\bar{y} < 1.5 \times 10^{-5}$ or a chemical potential $|\mu| < 9 \times 10^{-5}$ (Fixsen et al. 1996). *COBE* also demonstrated that the background contains small brightness fluctuations induced by density perturbations at decoupling with the character expected from simple inflation models (Gorski et al. 1996; Hinshaw et al. 1996; Wright et al. 1996).

More recently, *WMAP* has measured the power spectrum of these fluctuations over a wide range of multipole orders, l , and confirmed the existence of the peak in the power spectrum at $l \approx 200$, which the BOOMERanG (de Bernardis et al. 2000) and MAXIMA (Hanany et al. 2000) experiments used to show that the Universe is close to flat (Jaffe et al. 2001). Fits to the *WMAP* power spectrum have determined several cosmological parameters with good accuracy, notably the density parameter in baryons, $\Omega_b = 0.047 \pm 0.006$, the density parameter in matter, $\Omega_m = 0.29 \pm 0.06$, and the total density parameter $\Omega_{\text{total}} = 1.02 \pm 0.02$ (Bennett et al. 2003; Spergel et al. 2003). This review will adopt a value 72 ± 2 km s⁻¹ for the Hubble constant, derived from the *WMAP* results and the Hubble Key Project (Freedman et al. 2001), and will ignore the contribution of neutrinos to the Universe's dynamics since the *WMAP* results suggest that Ω_ν is negligible.

M. Birkinshaw

Additional brightness structures are induced in the microwave background radiation by massive objects between the epoch of decoupling and the present. The most important of these brightness structures is the thermal Sunyaev-Zel'dovich effect (Sunyaev & Zel'dovich 1972), which arises from the inverse-Compton scattering of the microwave background radiation by hot electrons in cluster atmospheres. Several other, but lower-amplitude, structures are also induced by clusters. Recent attention has focussed on those generated by the kinematic Sunyaev-Zel'dovich effect and the Rees-Sciama effect (Rees & Sciama 1968), particularly in the version that arises from the motions of clusters of galaxies across the line of sight (Pyne & Birkinshaw 1993; Molnar & Birkinshaw 2000).

The thermal Sunyaev-Zel'dovich effect was first detected at a high level of significance in 1978 (Birkinshaw, Gull, & Northover 1978). As instrumentation developed through the 1980's and 1990's it became a routine matter to measure the Sunyaev-Zel'dovich effects of the richest clusters of galaxies (e.g., Myers et al. 1997). Nevertheless, the use of the effect to explore the physics of the intracluster medium is still in its infancy because measurements remain slow. This has often led to reports about the effect, from individual clusters, rather than papers giving measurements for substantial cluster samples. With the development of dedicated telescopes the situation is now changing, and the effect is becoming an important feature of cluster studies.

In this review I describe the physics underlying the Sunyaev-Zel'dovich effect (§ 1.2), and then show how measurements of the effect can be used to extract quantities of physical interest about the clusters and the gas that they contain in a relatively model-independent way (§ 1.3) before describing the methods used to measure the effect and their limitations and future prospects (§ 1.4). There have been several reviews of the Sunyaev-Zel'dovich effect in recent years (Rephaeli 1995a; Birkinshaw 1999; Carlstrom, Holder, & Reese 2002), and these should be read to gain a more complete picture of Sunyaev-Zel'dovich effect research.

1.2 The Physics of the Sunyaev-Zel'dovich Effect

1.2.1 The Thermal Sunyaev-Zel'dovich Effect

The Sunyaev-Zel'dovich effects arise because hot electrons in the atmospheres of clusters of galaxies provide a significant optical depth to microwave background photons. A cluster of galaxies containing an X-ray emitting atmosphere with a electron temperature $T_e = 7 \times 10^7$ K ($k_B T_e = 6$ keV) and average electron density $\bar{n}_e = 10^3$ m⁻³ will have an optical depth for inverse-Compton scattering of

$$\tau_e = \bar{n}_e \sigma_T L \approx 10^{-2} , \quad (1.1)$$

where $\sigma_T = 6.65 \times 10^{-29}$ m² is the Thomson scattering cross-section, for a path length $L \approx 1$ Mpc through the cluster. Since electrons in the intracluster medium have higher mean energies than the photons, the 1% of the photons that are scattered gain energy on average. The mean fractional frequency change in a scattering is

$$\frac{\Delta\nu}{\nu} = \frac{k_B T_e}{m_e c^2} \approx 10^{-2} , \quad (1.2)$$

so that the fractional change in the specific intensity of the microwave background radiation, as seen through the cluster, relative to directions far from the cluster, is

$$\frac{\Delta I_\nu}{I_\nu} \propto \tau_e \frac{\Delta\nu}{\nu} \sim 10^{-4} . \quad (1.3)$$

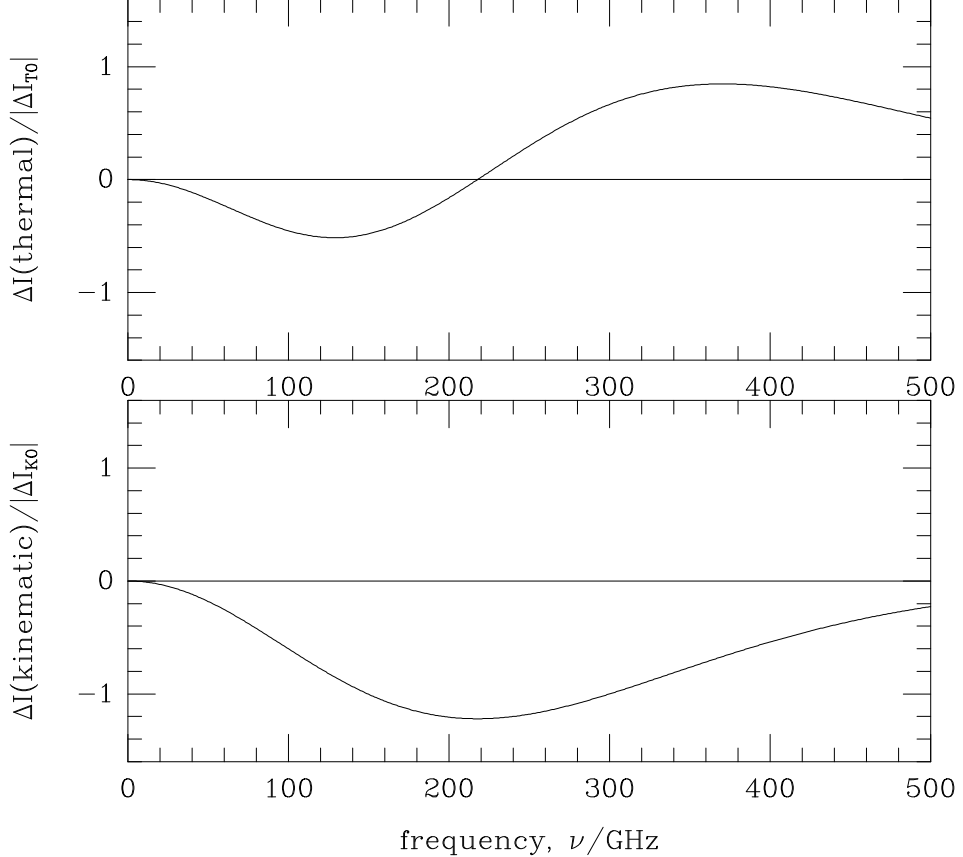


Fig. 1.1. The thermal (upper plot) and kinematic (lower plot) Sunyaev-Zel'dovich effects as functions of frequency, expressed in terms of the specific intensity change, ΔI_ν , that they produce. The largest negative and positive intensity changes in the thermal effect occur at 129 and 370 GHz, while the zero of the thermal effect and the largest negative kinematic effect occur at 218 GHz.

In the Rayleigh-Jeans part of the microwave background spectrum, where $I_\nu \propto \nu^2$, the constant of proportionality is -2 . The full spectrum of the thermal effect is shown in the upper panel of Figure 1.1 in terms of the specific intensity change, ΔI_ν , normalized by

$$\Delta I_{T0} = \frac{2h}{c^2} \left(\frac{k_B T_{\text{rad}}}{h} \right)^3 y \quad , \quad (1.4)$$

where the Comptonization parameter,

$$y = \int n_e \sigma_T dz \left(\frac{k_B T_e}{m_e c^2} \right) \quad , \quad (1.5)$$

measures the strength of the scattering

The spectrum in Figure 1.1 has an unusual shape for an astronomical source. Below about 218 GHz (the frequency of peak intensity of the microwave background) clusters of galaxies

appear as decrements, while at higher frequencies they are brightness enhancements. Even weak thermal Sunyaev-Zel'dovich effects could be identified against the background of primary fluctuations by observing over a wide range of frequencies and making use of this strong spectral signature. This will be possible with, for example, the data from the *Planck* satellite (Trauber 2001).

At low electron temperatures the spectrum of the thermal Sunyaev-Zel'dovich effect is independent of T_e , but as $k_B T_e$ rises above about 5 keV, the increasing fraction of electrons with speeds approaching the speed of light causes significant spectral modifications from relativistic effects (Rephaeli 1995b). In the limit of extreme relativistic electrons the spectrum becomes that of the (inverted) microwave background itself, since scattered photons are moved to energies far outside the microwave band. This nonthermal Sunyaev-Zel'dovich effect has been discussed as a probe of radio galaxy electron populations (McKinnon, Owen, & Eilek 1990), but is better observed from the scattered photons in the X-ray band than in the unscattered photons of the radio band (e.g., Hardcastle et al. 2002).

The amplitude of the thermal Sunyaev-Zel'dovich effect can be expressed in terms of the change in total intensity, ΔI_ν , at frequency ν , the change in the apparent thermodynamic temperature of a Planckian spectrum, ΔT_ν , or the brightness temperature change

$$\Delta T_{\text{RJ},\nu} = \frac{c^2}{2k_B\nu^2} \Delta I_\nu = f_T(\nu) T_{\text{rad}} y \quad , \quad (1.6)$$

where the spectral function $f_T(\nu)$, in the limit of low T_e , has the Kompaneets form

$$f_T(\nu) = \frac{x^2 e^x}{(e^x - 1)^2} \left(x \coth \left(\frac{1}{2}x \right) - 4 \right) \quad , \quad (1.7)$$

and

$$x = \frac{h\nu}{k_B T_{\text{rad}}} \quad (1.8)$$

is a dimensionless measure of frequency.

It is clear from Equation 1.6 that the brightness temperature effect depends only on quantities intrinsic to the cluster, and is therefore redshift independent. This property of redshift independence means that clusters of galaxies can be studied in the thermal Sunyaev-Zel'dovich effect at any redshift where they have substantial atmospheres. The wide range of redshifts over which the thermal Sunyaev-Zel'dovich effect can be seen makes the effect an important probe of cluster evolution.

Practical telescope systems observe a quantity that is a fraction of the total flux density of a cluster, with the fraction depending principally on the method of observation and the cluster angular size, and often being almost constant over a wide range of redshifts (as in Fig. 1.4). The total cluster flux density at frequency ν is

$$\Delta S_\nu = \int \Delta I_\nu d\Omega \propto \frac{\int n_e T_e dV}{D_A^2} \quad , \quad (1.9)$$

where the integrals are over the solid angle of the cluster and the cluster volume. ΔS_ν decreases as the inverse square of the angular diameter distance, D_A , rather than the inverse square of the luminosity distance. This can be thought of as indicating that Sunyaev-Zel'dovich effect luminosities increase as $(1+z)^4$, because the luminosity depends on the energy density of the cosmic microwave background that is available to be scattered. If a

given cluster of galaxies were to be moved from low to high redshift, its flux density would first decrease, and then increase beyond the redshift of minimum angular size, or $z = 1.62$ in the Λ CDM cosmology adopted here.

Thus at mm wavelengths, the brightest sources in the sky would be clusters of galaxies if clusters had the same atmospheres in the past as they have today. That the brightest mm-wave sources are not clusters does not place a strong constraint on cluster evolution because $D_A(z)$ is a weak function of redshift at $z > 1.6$: from $z = 1.6$ to 9.8 it decreases by only a factor of 2.

1.2.2 *The Kinematic Sunyaev-Zel'dovich Effect*

If a cluster of galaxies is not at rest in the Hubble flow then the pattern of radiation illuminating the atmosphere in its rest frame is anisotropic, and scattering adds a kinematic Sunyaev-Zel'dovich effect to the thermal effect described in § 1.2.1 (Sunyaev & Zel'dovich 1972; Rephaeli & Lahav 1991). The kinematic effect has an amplitude that is proportional to the cluster's peculiar (redshift-direction) velocity, and has a spectrum that is that of the primary perturbations in the microwave background radiation (Fig. 1.1, lower panel), where

$$\Delta I_{K0} = \tau_e \frac{v_z}{c} \frac{2h}{c^2} \left(\frac{k_B T_{\text{rad}}}{h} \right)^3 . \quad (1.10)$$

The similarity of spectrum makes it difficult to distinguish the kinematic effect from primary fluctuations in the microwave background radiation. This is especially a problem since the kinematic effect is smaller than the thermal effect by a factor

$$\frac{\Delta T_{\text{RJ,kinematic}}}{\Delta T_{\text{RJ,thermal}}} = 0.085 \left(v_z / 1000 \text{ km s}^{-1} \right) \left(k_B T_e / 10 \text{ keV} \right)^{-1} \quad (1.11)$$

at low frequencies. Observation near the null of the thermal Sunyaev-Zel'dovich effect, at $\nu_0 = 218$ GHz, gives the greatest contrast for the kinematic effect, but it is still a small quantity compared to the confusion from primary structure in the microwave background radiation on the angular scales of interest (a few arcmin). This limits the velocity accuracy attainable for any cluster of galaxies at moderate redshift to about $\pm 150 \text{ km s}^{-1}$, even with perfect data.

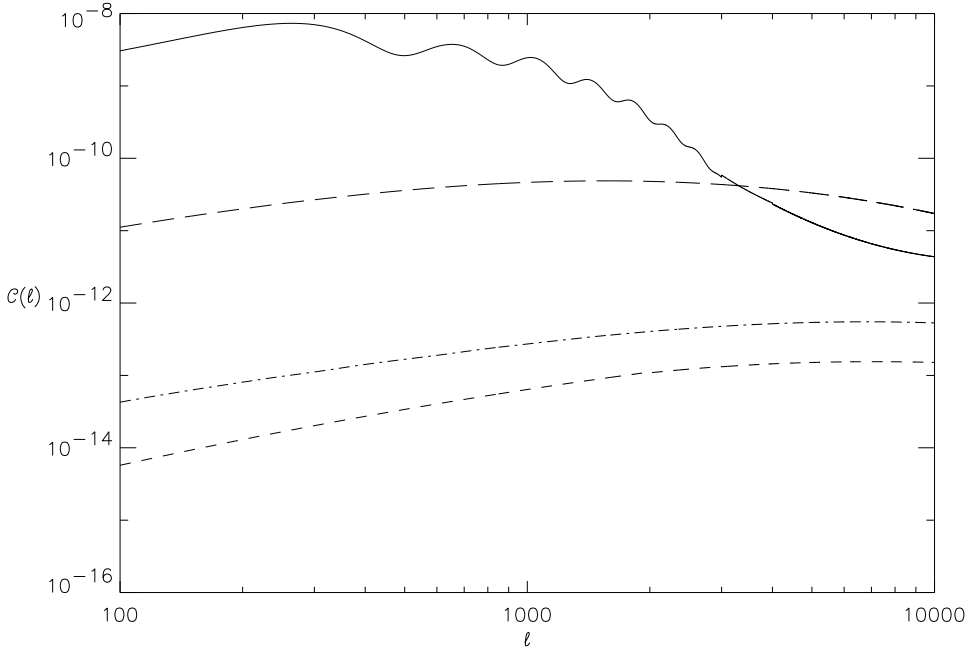
The relative contributions of the thermal and kinematic Sunyaev-Zel'dovich effects to the power spectrum of the microwave background radiation have been calculated by a number of authors (e.g., da Silva et al. 2000; Molnar & Birkinshaw 2000; Springel, White, & Hernquist 2000). The thermal Sunyaev-Zel'dovich effect is expected to dominate on sufficiently small angular scales (Fig. 1.2), but on average the kinematic effect makes a contribution only about 1% that of the thermal effect. Both effects are larger than the lensing effect of moving clusters of galaxies.

1.3 **Uses of the Sunyaev-Zel'dovich Effect in Cluster Studies**

1.3.1 *Thermal Energy Content of Clusters*

The total flux density of the thermal Sunyaev-Zel'dovich effect from a cluster is given by Equation 1.9, which can be rewritten

$$\Delta S_\nu \propto \frac{U_e}{D_A^2} , \quad (1.12)$$



vskip 0pt

Fig. 1.2. The lensed primary power spectrum for a Λ CDM cosmology with $\Omega_\Lambda = 0.8$, $\Omega_{\text{CDM}} = 0.2$, and $n = -1.4$ (solid line), with the power spectrum expected from the thermal Sunyaev-Zel'dovich effect (long dashed line), kinematic Sunyaev-Zel'dovich effect (dash-dot line), and the Rees-Sciama effect from moving clusters (short dashed line) effects. (From Molnar & Birkinshaw 2000.)

where U_e is the total thermal energy content of electrons in the intracluster medium. That is, measurements of the redshift and thermal Sunyaev-Zel'dovich effect of a cluster allow us to infer the thermal energy content of the intracluster medium without needing to know the structure of the density or temperature of this gas.

The thermal Sunyaev-Zel'dovich effect therefore can be used as a calorimeter, measuring the integrated heating to which the cluster gas has been subjected, although a correction has to be made for energy lost by (principally X-ray) radiation (Lapi, Cavaliere, & De Zotti 2003). If the gas is approximately in hydrostatic equilibrium in the cluster, this thermal energy content should be a good measure of the gravitational energy of the cluster, and so a survey for thermal Sunyaev-Zel'dovich effects should naturally pick out the deepest gravitational potential wells in the Universe, provided that the ratio of intracluster gas mass to total mass does not vary too much from cluster to cluster.

1.3.2 The Baryonic Mass Content of Clusters

If the integrated flux density of the thermal Sunyaev-Zel'dovich effect and the X-ray spectrum of a cluster are both available, then we can rewrite Equation 1.12 as

$$\Delta S_\nu \propto \int d\Omega \int dz n_e T_e \propto N_e \overline{T_e} \quad . \quad (1.13)$$

If the mass-weighted mean electron temperature, $\overline{T_e}$, can be approximated by the emission-measure weighted temperature measured by X-ray spectra, then ΔS_ν measures the total electron count in the intracluster medium, N_e . A metallicity measurement for the gas, again from the X-ray spectrum, allows N_e to be converted into the baryonic mass of the intracluster medium. This is usually far larger than the stellar mass content, and so is a good measure of the total baryonic content of the cluster. X-ray imaging data can be used to estimate cluster total masses, using the assumption of hydrostatic equilibrium (Fabricant, Lecar, & Gorenstein 1980), and so the baryonic mass fraction of clusters can be measured.

Since X-ray images and spectra, and Sunyaev-Zel'dovich effects, can be measured from massive clusters to $z \approx 1$, a history of the baryonic mass fraction of clusters can be constructed, although this is currently biased to the high-mass end of the cluster population. The result, for the 10–20 clusters for which this has been done to date (Grego et al. 2001), is that this ratio does not change significantly with redshift, remaining close to the result $\Omega_b/\Omega_m = 0.16 \pm 0.04$ deduced from the *WMAP* results or primordial nucleosynthesis. This suggests that clusters are fair samples of the mass of the Universe out to the largest redshifts at which this test has been applied: there is no strong segregation of dark and baryonic matter during cluster collapse.

1.3.3 Cluster Lensing and the Sunyaev-Zel'dovich Effects

It is interesting to consider the possibility of combining Sunyaev-Zel'dovich effect data with gravitational lensing, rather than X-ray, data, to study baryonic mass fractions. If the ellipticity field $\epsilon_i(\theta)$ has been measured (and corrected to estimate the shear distortion field), then the surface mass density of a lensing cluster is given by an integral

$$\Sigma = -\frac{1}{\pi} \Sigma_{\text{crit}} \int d^2\theta' K_i(\theta', \theta) \epsilon_i(\theta') \quad , \quad (1.14)$$

where Σ_{crit} is the critical surface density, and the kernels K_i are angular weighting functions. Clearly, the surface mass density is a linear (though nonlocal) function of the observable quantity, $\epsilon_i(\theta)$. Since the Sunyaev-Zel'dovich effect is a linear measure of the projected baryonic mass density (if the cluster is isothermal), the ratio of a Sunyaev-Zel'dovich effect map to a mass map derived from lensing should give a good measure of the (projected) radial dependence of baryonic mass fraction. This should be consistent with the result obtained by applying the standard assumption of hydrostatic equilibrium to the X-ray data, but is less susceptible to errors arising from the unknown structure of the cluster along the line of sight.

The earliest suggestion of the use of lensing and Sunyaev-Zel'dovich effect data together to study clusters appears to have been made by Ostriker & Vishniac (1986) in the context of the quasar pair 1146+111B, C, but little work on the comparison has been done to date, although Doré et al. (2001) and Zaroubi et al. (2001) have shown that the addition of lensing data allows the three-dimensional structure of clusters to be investigated.

A comparison of lensing and X-ray derived masses has been made for the inner 250 kpc of cluster CL 0016+16 (Fig. 1.3) by Worrall & Birkinshaw (2003). Within this radius, set by the limited lensing data, the masses are

$$M_{\text{tot}} = (2.7 \pm 0.9) \times 10^{14} M_\odot \quad (1.15)$$

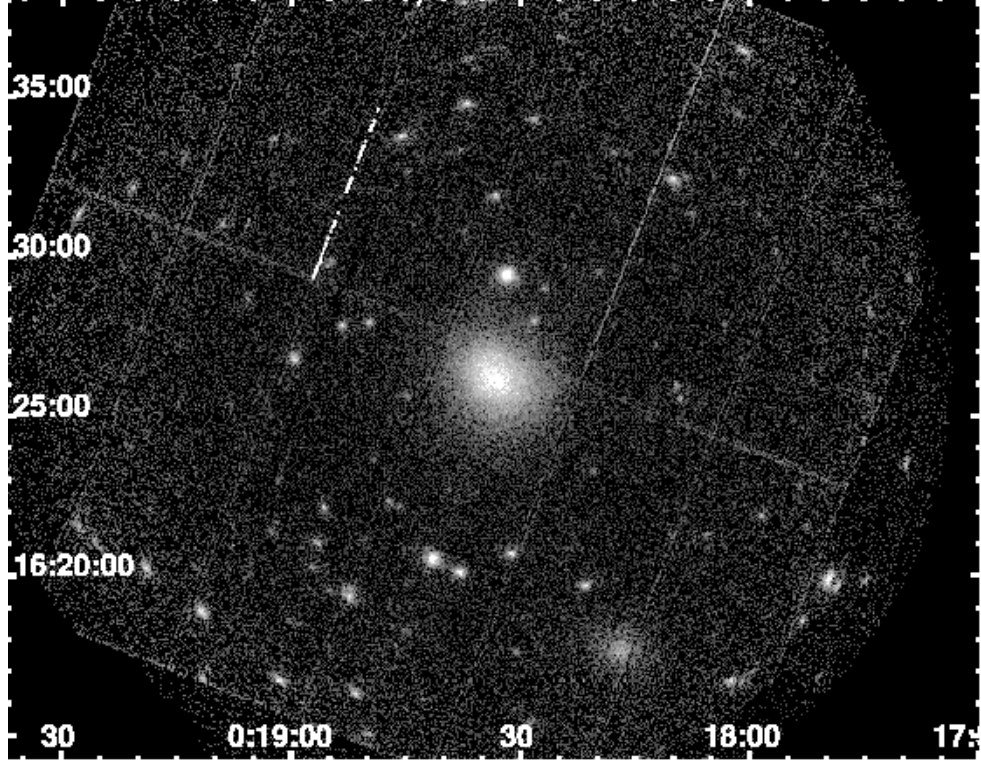


Fig. 1.3. A vignetting-corrected 0.3–5.0 keV image of CL 0016+16, from an *XMM-Newton* observation (Worrall & Birkinshaw 2003). A quasar 3' north of the cluster, and a second cluster, 9' to the south-west, are at similar redshifts to CL 0016+16.

and

$$M_{\text{tot}} = (2.0 \pm 0.1) \times 10^{14} M_{\odot} \quad , \quad (1.16)$$

found from lensing (Smail et al. 1997, converted to our cosmology) and X-ray data, respectively. The results agree to within the limited accuracy of the lensing mass. A combination of these data with the central Sunyaev-Zel'dovich effect for the cluster, of -1.26 ± 0.07 mK, then leads to a distance-independent measure of the baryonic mass fraction within the central part of the cluster of 0.13 ± 0.02 , close to the value implied by cosmological parameters.

1.3.4 Cluster Structures

The structures of cluster atmospheres are generally studied from their X-ray images. The X-ray surface brightness

$$b_X \propto \int n_e^2 \Lambda(T_e) dz \quad , \quad (1.17)$$

where $\Lambda(T_e)$ is the emissivity function. The X-ray image can be inverted to derive an electron density profile, $n_e(r)$, for the cluster atmosphere under assumptions about the shape of the

atmosphere and the absence of clumping, which would cause $\overline{n_e^2} > (\overline{n_e})^2$. Since the Sunyaev-Zel'dovich effects are a projection of n_e , rather than the more complicated quantity $n_e^2 \Lambda(T_e)$, they should give a cleaner measure of the structure of the atmosphere. However, the restricted angular dynamic range of measurements of Sunyaev-Zel'dovich effects (§ 1.4), and lower signal-to-noise ratio and angular resolution of Sunyaev-Zel'dovich effect maps relative to what is possible with long X-ray exposures, means that X-ray based structures are superior to those derived entirely from the Sunyaev-Zel'dovich effects. Furthermore, since the Sunyaev-Zel'dovich effects are line-of-sight integrals of electron pressure, they are insensitive to subsonic structures within a cluster, such as cold fronts, which are easily seen on *Chandra* X-ray images (e.g., Markevitch et al. 2000).

The different n_e dependencies of the Sunyaev-Zel'dovich effect and X-ray surface brightness also implies that clusters of galaxies have larger angular sizes in Sunyaev-Zel'dovich effects than in the X-ray, and that the X-ray emission is more sensitive to cluster cores, while the Sunyaev-Zel'dovich effects are more weighted toward the low-density envelopes. However, the low surface brightness of cluster envelopes, and low signal-to-noise ratio even in the centers of most Sunyaev-Zel'dovich effect maps, means that the X-ray data are superior out to the largest radii to which gas has been detected.

1.3.5 Cluster Distances

Perhaps the most widely discussed use of the thermal Sunyaev-Zel'dovich effect has been to measure the distances of clusters of galaxies. In its simplest form, the method is to compare the X-ray surface brightness of a cluster on some fiducial line of sight,

$$b_{X0} \propto n_{e0}^2 \Lambda(T_{e0}) L \quad , \quad (1.18)$$

with the thermal Sunyaev-Zel'dovich effect on the same line of sight,

$$\Delta T_{RJ,0} \propto n_{e0} T_{e0} L \quad , \quad (1.19)$$

and eliminate the scale (perhaps central) electron density in the cluster and find an absolute measurement of the path length along some fiducial line of sight

$$L \propto \frac{\Delta T_{RJ,0}^2}{b_{X0}} \cdot \frac{\Lambda(T_{e0})}{T_{e0}^2} \quad . \quad (1.20)$$

This path length can then be compared with the angular size of the cluster to infer the cluster's angular diameter distance, under the assumption that the cluster is spherical. This technique has been used for a number of clusters (e.g., Hughes & Birkinshaw 1998; Mason, Myers, & Readhead 2001; Reese et al. 2002). A recent recalculation of the distance to CL 0016+16 (Fig. 1.3) using this technique gave $D_A = 1.16 \pm 0.15$ Gpc (Worrall & Birkinshaw 2003), and implies a Hubble constant of $68 \pm 8 \pm 18 \text{ km s}^{-1} \text{ Mpc}^{-1}$.

While single cluster distances are likely to be error-prone, because of their unknown three-dimensional shapes (and hence the large systematic error on the result for CL 0016+16), a suitably chosen sample of clusters, without an orientation bias, can be used to map the Hubble flow to $z \approx 1$, and hence to measure a number of cosmological parameters. Molnar, Birkinshaw, & Mushotzky (2002) have shown that a set of about 70 clusters could provide useful measure of the equation-of-state parameter, w , as well as the Hubble constant. A recent review of the state of measurement of $D_A(z)$ using this technique is given by Carlstrom et al. (2002).

It is critical that the absolute calibrations of the X-ray and Sunyaev-Zel'dovich effect data are excellent, and that cluster substructure is well modeled, if distances are to be estimated in this way. Since clusters are relatively young structures, and likely to be changing significantly with redshift, variations in the amount of substructure with redshift might be a significant source of systematic error. High-quality X-ray imaging and spectroscopy are therefore essential if the distances obtained are to be reliable.

Finally, a crucial element of this technique is that the set of clusters used should be free from any biasing selection effect. Perhaps the most important such effect is that of orientation: if clusters are selected by any surface brightness sensitive criterion, then they will tend to be preferentially aligned relative to the line of sight. Since the distance measurement technique relies on comparing the line-of-sight depth of the cluster, L , with the cross line-of-sight angular size, θ , such a selection will inevitably induce a bias into the measured $D_A(z)$ function.

Clumping of the intracluster medium and a number of other problems can also cause biases in the results. Comprehensive reviews of such biases can be found in most papers on Hubble constant measurements using this technique, and in Birkinshaw (1999).

1.3.6 Cluster Peculiar Velocities

The kinematic Sunyaev-Zel'dovich effect (§ 1.2.2) is heavily confused by primary anisotropies in the microwave background radiation since cluster peculiar velocities are expected to be less than 100 km s^{-1} . It seems likely, therefore, that measurement of the kinematic effect will only be possible on a statistical basis, by comparing the brightness of the microwave background radiation toward the clusters of galaxies with positions in the field. Since the kinematic effect, like the thermal effect, is redshift independent, such a statistical measurement would be an important check on the changing velocities of clusters with redshift as structure develops. Efforts to measure the kinematic effect continue, although only relatively poor limits on cluster velocities, of order 1000 km s^{-1} , have been obtained to date (Holzapfel et al. 1997a; LaRoque et al. 2003b).

1.3.7 Cluster Samples

Since the Sunyaev-Zel'dovich effects are redshift-independent in ΔT_{RJ} terms, and the observable ΔS_ν are almost redshift-independent, it follows that Sunyaev-Zel'dovich effect surveys should be more effective than X-ray or optical surveys at detecting clusters of galaxies at large redshift. Such samples of clusters, selected by their Sunyaev-Zel'dovich effects, will be unusually powerful in being almost mass limited, and counts of the number of such clusters as a function of redshift provide a good method of measuring σ_8 (Fan & Chiueh 2001).

Such samples are also ideal for work on the distance scale, and hence the measurement of the equation-of-state parameter, w .

1.4 Instruments and Techniques

Many observations of the thermal Sunyaev-Zel'dovich effect have followed its first reliable detection, in Abell 2218 (Birkinshaw et al. 1978). While the earliest observations were made with single-dish radiometers, more recently work has been done with interferometers and bolometer arrays. The quality of the observational data is advancing rapidly, so

M. Birkinshaw

that the review of the observational situation that I wrote in 1999 (Birkinshaw 1999) grossly underrepresents the number of good detections and images of the effect.

The most effective observations of the Sunyaev-Zel'dovich effects over the past few years have used interferometers, notably the Ryle telescope (Jones et al. 1993) and the BIMA and OVRO arrays (Carlstrom, Joy, & Grego 1996). Since the thermal Sunyaev-Zel'dovich effects of rich clusters typically have angular sizes exceeding $1'$, most of the correlated signal appears on the shortest ($< 2000\lambda$) baselines. These baselines are usually underrepresented in the interferometers, so that all these instruments had to be retrofitted by increasing the observing wavelength, λ , or altering the array geometry. The effectiveness of the changes is demonstrated by the large number of high signal-to-noise ratio detections of clusters of galaxies that interferometers have produced (e.g., Joy et al. 2001; Cotter et al. 2002; Grainge et al. 2002).

The major advantage of interferometers is their ability to reject contaminating signals from their surroundings and the atmosphere, and to spatially filter the data to exclude radio point sources in the fields of the clusters. Extremely long interferometric integrations are possible before parasitic signals degrade the data. The limitation, at present, is that the retrofitted arrays are not ideally matched to the purpose of mapping the Sunyaev-Zel'dovich effect. This limitation is being addressed by the construction of a new generation of interferometers, including AMI (Kneissl et al. 2001), SZA (Mohr et al. 2002), and AMiBA (Lo et al. 2001), which will have enough sensitivity to undertake deep blank-field surveys for clusters at $z > 1$.

Single-dish radiometer systems, particularly when equipped with radiometer arrays, are efficient for finding strong Sunyaev-Zel'dovich effects. Their large filled apertures can integrate the signal over much of the solid angle of a cluster. However, spillover and residual atmospheric noise limit the length of useful integrations and hence the sensitivity that can be achieved (Birkinshaw & Gull 1984). Since practical systems always involve differencing between on-source and off-source sky regions, this technique, just as interferometry, is sensitive only to clusters smaller than some maximum angular size, and hence at sufficiently large redshift. Finally, there is no simple way of removing the signals of contaminating (and often variable) radio sources that appear superimposed on the Sunyaev-Zel'dovich effect. This further restricts the set of clusters that can be observed effectively.

Modern antennas provide new opportunities for radiometer systems since they have superior spillover characteristics and can be equipped with radiometer arrays. The 100-meter Green Bank Telescope is an obvious example, and the OCRA project (§ 1.4.2) is intending to provide a fast survey capability for this and other large telescopes.

Bolometers are capable of measuring the spectrum of the Sunyaev-Zel'dovich effect above ~ 90 GHz, and could separate the thermal Sunyaev-Zel'dovich effect from the associated kinematic effect or from primary anisotropy confusion. The intrinsic sensitivity of bolometers should allow fast measurements of targeted clusters, or high-speed surveys of large regions of sky. However, bolometers are exposed to a high level of atmospheric and other environmental signals, and so the differencing scheme used to extract sky signals from the noise must be of high quality.

There have been two attempts to use the spectral capability of bolometers to determine cluster peculiar velocities (Holzapfel et al. 1997a; LaRoque et al. 2003b), and a similar experiment can use the spectral distortion of the thermal effect to measure the temperature of the microwave background radiation in remote parts of the Universe and test whether

M. Birkinshaw

$T_{\text{rad}} \propto (1+z)$ (Battistelli et al. 2002). Newer bolometer arrays, such as BOLOCAM (Glenn et al. 1998) and ACBAR (Romer et al. 2001), should allow fast surveys for clusters and could make confusion-limited measurements of the cluster velocity if the flux scale near 1 mm is well calibrated.

1.4.1 Recent Advances

A major advance over the past few years has been the change from making and reporting Sunyaev-Zel'dovich effects for individual clusters to reporting for samples of clusters. The samples most favored are based on X-ray surveys (e.g., Mason et al. 2001; LaRoque et al. 2003a), and can be assumed to be orientation-independent provided that the selection is at X-ray fluxes far above the sensitivity limit of the survey. The combination of good X-ray and Sunyaev-Zel'dovich effect data is leading to reliable results for baryon fractions and the Hubble constant.

The next improvement will clearly be to obtain samples of clusters selected entirely in the Sunyaev-Zel'dovich effect, on the basis of blind surveys. Such surveys require sensitive, arcminute-scale, instruments capable of covering many deg^2 of sky in a reasonable length of time — a good first target would be to cover 10 deg^2 to a sensitivity limit $\Delta T_{\text{RJ}} \approx 100 \mu\text{K}$, yielding a sample of tens of clusters selected only through their Sunyaev-Zel'dovich effects. Such cluster samples would be ideal for cosmological purposes, since they would be almost mass limited. Since the observable thermal Sunyaev-Zel'dovich effect depends linearly on the properties of clusters, and on the angular diameter distance, which is a slow function of redshift for $z \approx 1$, a cluster of a given mass can be detected with almost the same efficiency at any redshift > 0.5 . This is illustrated for the OCRA instrument (Browne et al. 2000) in Figure 1.4.

Many of the new projects are aimed at blind surveys of the microwave background sky to find Sunyaev-Zel'dovich effects, and hence complete cluster samples. Figure 1.5 compares the survey speeds of these projects, ranging from radiometer and bolometer arrays (OCRA, BOLOCAM) to interferometers (AMiBA, SZA, AMI). AMiBA and OCRA are discussed in more detail in the next section.

1.4.2 Two New Projects: AMiBA and OCRA

AMiBA, the Array for Microwave Background Anisotropy, is described by Lo et al. (2001). It is a platform-based system, operating at 95 GHz with a bandwidth of 20 GHz, with up to 19 1.2-m antennas, providing an $11'$ field of view and approximately $2'$ angular resolution. Its flux density sensitivity, 1.3 mJy per beam in 1 hour, makes it a highly effective interferometer for surveys: a 3-hour observation suffices to detect a $z = 0.5$ cluster with mass $2.7 \times 10^{14} M_{\odot}$ at 5σ , and clusters with about a third of this mass could be detected well above the confusion limit in longer integrations.

A trial platform carrying two smaller antennas has been operating on Mauna Loa for some months, and various aspects of the system are being tried out and debugged. AMiBA should be operational in the 2003/4 winter season for studies of primary structure in the microwave background radiation, and full Sunyaev-Zel'dovich effect operations should start about 1 year later.

The high density of short antenna-antenna spacings and the 3-mm operating wavelength make AMiBA the most sensitive of the planned interferometers. However, AMI at 15 GHz (Kneissl et al. 2001), the SZA at 30 GHz (Mohr et al. 2002), and AMiBA at 95 GHz have

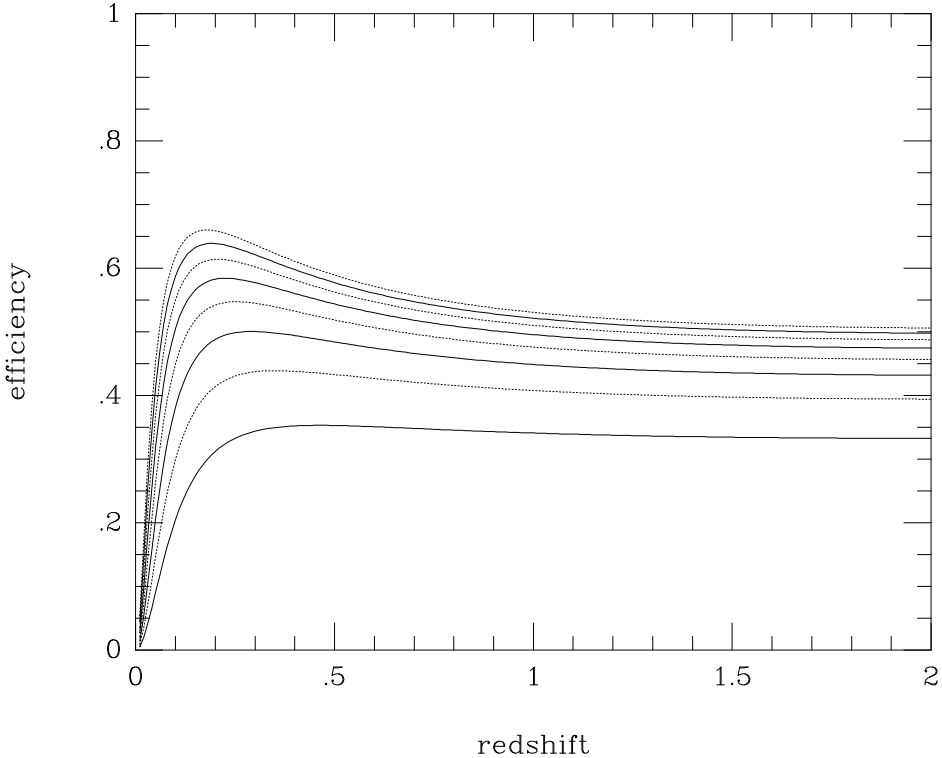


Fig. 1.4. The relative sensitivity of observations of the thermal Sunyaev-Zel'dovich effect in a cluster of galaxies as a function of differencing angle (from 1.5' to 5.0' from the bottom to the top curve) and redshift for the One Centimeter Radiometer Array (OCRA; Browne et al. 2000). Note the flatness of the sensitivity function at $z > 0.5$ for any differencing angle.

usefully complementary angular resolutions and operating frequencies. Although the spread of frequencies provided by these three systems is inadequate for useful spectral work, to separate primary anisotropies and kinematic effects from the thermal signal, it is sufficient to provide a control against nonthermal radio sources, and an important cross-check on cluster counts.

Several thousand individual pointings with AMiBA would be needed for a shallow survey of the entire 64 deg² *XMM-Newton* survey field (Pierre et al. 2001). While most of the $\sim 10^3$ Sunyaev-Zel'dovich effect detections expected will correspond to X-ray clusters, a comparison of the *XMM-Newton* and AMiBA detection functions shows that AMiBA will be better at detecting clusters beyond $z = 0.7$, and could find clusters with X-ray luminosities $> 4 \times 10^{43}$ erg s⁻¹ (in 0.5–10 keV) to $z > 2$ for later, deeper, X-ray and infrared follow-up.

While AMiBA has the interferometric advantages of rejecting contaminating environmental signals, high sensitivity and fast survey speed are better achieved by radiometer arrays. OCRA, the One Centimeter Radiometer Array (Browne et al. 2000), has been designed to make use of recent advances in radiometer technology to perform wide-field surveys for Sunyaev-Zel'dovich effects and radio sources.

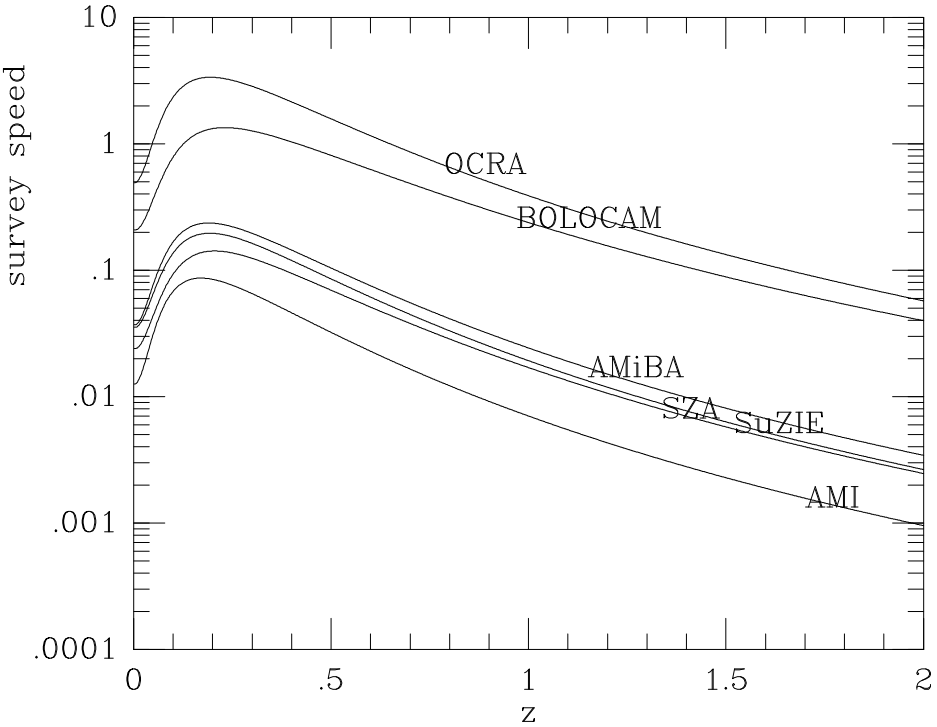


Fig. 1.5. The relative speeds of several future Sunyaev-Zel'dovich effect instruments, as a function of redshift, for a model in which the cluster gas evolves in a non self-similar fashion. The experiments shown are OCRA (Browne et al. 2000; § 1.4.2), BOLOCAM (Glenn et al. 1998), AMiBA (Lo et al. 2001; § 1.4.2), SZA (Mohr et al. 2002), SuZIE (Holzapfel et al. 1997b), and AMI (Kneissl et al. 2001).

OCRA is an array of ~ 100 30-GHz radiometers, based on *Planck* technology, housed in a single cryostat at the secondary (or tertiary) focal plane of a large antenna, and providing $1'$ beams with $\sim 3'$ beam separations. Each radiometer has excellent flux density sensitivity at 30 GHz. This is a large and expensive system, and two preliminary (but scientifically useful) versions of OCRA will be used before OCRA is built.

The prototype, OCRA-p, is a two-beam system now being tested on the Torun 32-m radio telescope. With a system temperature below 40 K, we expect to achieve a flux density sensitivity of 5 mJy in 10 s provided that the atmospheric noise is well controlled. OCRA-p will be followed by a FARADAY project receiver with eight beams, which uses MMICs on InP substrates, and which is funded by a European Union grant. This receiver is currently under construction and will be in use in about a year. It will achieve a significant improvement in mapping speed over OCRA-p, though still be a factor ~ 10 slower than OCRA itself.

OCRA will be an extremely fast instrument for finding high-redshift clusters. A comparison of its mapping speed with some other systems is shown in Figure 1.5. While OCRA is more susceptible to radio source confusion than AMiBA (indeed, the study of the radio

source population at 30 GHz is one aim of OCRA), recent work on the probability of detecting Sunyaev-Zel'dovich effects from clusters at 18.5 GHz (Birkinshaw, in preparation) suggests that the level of source confusion will not prevent OCRA from detecting most rich, distant clusters. Even the FARADAY receiver will be a highly competitive survey instrument.

1.5 Summary

The thermal Sunyaev-Zel'dovich effects of clusters of galaxies, expressed in brightness temperature terms, are redshift-independent measures of the thermal energy content of clusters: they are, effectively, calorimeters of energy releases in clusters after account is taken of the energy radiated by line and bremsstrahlung emission (principally in the X-ray band). With the assistance of X-ray and/or gravitational lensing data, the thermal Sunyaev-Zel'dovich effect measures a wide range of cluster properties, including distance.

Thermal Sunyaev-Zel'dovich effects are mass finders, with strong associations with rich clusters of galaxies, and should be good probes of the most massive structures that exist in the Universe at any redshift. Deep Sunyaev-Zel'dovich effect studies are therefore an excellent way of discovering the degree of cluster formation in the Universe to high redshift, and counts of clusters from forthcoming surveys should place strong constraints on the processes of cluster formation.

Two weaker Sunyaev-Zel'dovich effects, the kinematic and polarization effects, are also of interest, but are harder to measure. Both can give information about the speeds of clusters of galaxies, and hence the evolving dynamics of gravitating objects in the Universe, but both are subject to considerable confusion from primary structures in the microwave background radiation and are therefore likely to be detectable only in a statistical sense for populations of clusters.

Over the past 20 years, the thermal Sunyaev-Zel'dovich effect has gone from being a curiosity to a major tool for cosmology and cluster physics. Substantial results based on Sunyaev-Zel'dovich effect work are to be expected within the next 10 years.

References

Battistelli, E. S., et al. 2002, *ApJ*, 580, L101
 Bennett, C. L., et al. 2003, *ApJ*, submitted (astro-ph/0302207)
 Birkinshaw, M. 1999, *Phys. Rep.*, 310, 97
 Birkinshaw, M., & Gull, S. F. 1984, *MNRAS*, 206, 359
 Birkinshaw, M., Gull, S. F., & Northover, K. J. E. 1978, *Nature*, 185, 245
 Browne, I. W. A., Mao, S., Wilkinson, P. N., Kus, A. J., Marecki, A., & Birkinshaw, M. 2000, *Proc. SPIE*, 4015, 299
 Carlstrom, J. E., Holder, G. P., & Reese, E. D. 2002, *ARA&A*, 40, 643
 Carlstrom, J. E., Joy, M., & Grego, L. 1996, *ApJ*, 456, L75 (erratum: 461, L9)
 Cotter, G., Buttery, H. J., Das, R., Jones, M. E., Grainge, K., Pooley, G. G., & Saunders, R. 2002, *MNRAS*, 334, 323
 da Silva, A. C., Barbosa, D., Liddle, A. R., & Thomas, P. A. 2000, *MNRAS*, 317, 37
 de Bernardis, P., et al. 2000, *Nature*, 404, 955
 Dicke, R. H., Peebles, P. J. E., Roll, P. G., & Wilkinson, D. T. 1965, *ApJ*, 142, 414
 Doré, O., Bouchet, F. R., Mellier, Y., & Teyssier, R. 2001, *A&A*, 375, 14
 Fabricant, D., Lecar, M., & Gorenstein, P. 1980, *ApJ*, 241, 552
 Fan, Z., & Chiueh, T. 2001, *ApJ*, 550, 547
 Fixsen, D. J., Cheng, E. S., Gales, J. M., Mather, J. C., Shafer, R. A., & Wright, E. L. 1996, *ApJ*, 473, 576

M. Birkinshaw

Freedman, W. L., et al. 2001, *ApJ*, 553, 47

Glenn, J., et al. 1998, *Proc. SPIE*, 3357, 326

Gorski, K. M., Banday, A. J., Bennett, C. L., Hinshaw, G., Kogut, A., Smoot, G. F., & Wright, E. L. 1996, *ApJ*, 464, L11

Grainge, K., Jones, M. E., Pooley, G., Saunders, R., Edge, A., Grainger, W. F., & Kneissl, R. 2002, *MNRAS*, 333, 318

Grego, L., Carlstrom, J. E., Reese, E. D., Holder, G. P., Holzapfel, W. L., Joy, M. K., Mohr, J. J., & Patel, S. 2001, *ApJ*, 552, 2

Hanany, S., et al. 2000, *ApJ*, 545, L5

Hardcastle, M. J., Birkinshaw, M., Cameron, R. A., Harris, D. E., Looney, L. W., & Worrall, D. M. 2002, *ApJ*, 581, 948

Hinshaw, G., Banday, A. J., Bennett, C. L., Gorski, K. M., Kogut, A., Smoot, G. F., & Wright, E. L. 1996, *ApJ*, 464, L17

Holzapfel, W. L., Ade, P. A. R., Church, S. E., Mauskopf, P. D., Rephaeli, Y., Wilbanks, T. M., & Lange, A. E. 1997a, *ApJ*, 481, 35

Holzapfel, W. L., Wilbanks, T. M., Ade, P. A. R., Church, S. E., Fischer, M. L., Mauskopf, P. D., Osgood, D. E., & Lange, A. E. 1997b, *ApJ*, 479, 19

Hughes, J. P., & Birkinshaw, M. 1998, *ApJ*, 501, 1

Jaffe, A. H., et al. 2001, *Phys. Rev. Lett.*, 86, 3475

Jones, M., et al. 1993, *Nature*, 365, 320

Joy, M., et al. 2001, *ApJ*, 551, L1

Kneissl, R., Jones, M. E., Saunders, R., Eke, V. R., Lasenby, A. N., Grainge, K., & Cotter, G. 2001, *MNRAS*, 328, 783

Lapi, A., Cavaliere, A., & De Zotti, G. 2003, in *Carnegie Observatories Astrophysics Series*, Vol. 3: Clusters of Galaxies: Probes of Cosmological Structure and Galaxy Evolution, ed. J. S. Mulchaey, A. Dressler, & A. Oemler (Pasadena: Carnegie Observatories, <http://www.ociw.edu/ociw/symposia/series/symposium3/proceedings.html>)

LaRoque, S. J., et al. 2003a, *ApJ*, 583, 559

LaRoque, S. J., Carlstrom, J. E., Reese, E. D., Holder, G. P., Holzapfel, W. L., Joy, M., & Grego, L. 2003b, *ApJ*, in press (astro-ph/0204134)

Lo, K. Y., Chiueh, T., Liang, H., Ma, C. P., Martin, R., Ng, K.-W., Pen, U. L., & Subramanyan, R. 2001, in *IAU Symp. 201*, ed. A. N. Lasenby, A. W. Jones & A. Wilkinson (San Francisco: ASP), 31

Markevitch, M., et al. 2000, *ApJ*, 541, 542

Mason, B. S., Myers, S. T., & Readhead, A. C. S. 2001, *ApJ*, 555, L11

McKinnon, M. M., Owen, F. N., & Eilek, J. A. 1990, *AJ*, 101, 2026

Mohr, J. J., et al. 2002, in *AMiBA 2001: High-z Clusters, Missing Baryons, and CMB Polarization*, ed. L. W. Chen et al. (San Francisco: ASP), 43

Molnar, S., & Birkinshaw, M. 2000, *ApJ*, 537, 542

Molnar, S., Birkinshaw, M., & Mushotzky, R. F. 2002, *ApJ*, 570, 1

Myers, S. T., Baker, J. E., Readhead, A. C. S., Leitch, E. M., & Herbig, T. 1997, *ApJ*, 485, 1

Ostriker, J. P., & Vishniac, E. T. 1986, *Nature*, 322, 804

Penzias, A. A., & Wilson, R. W. 1965, *ApJ*, 142, 419

Pierre, M., et al. 2001, *ESO Messenger*, 105, 32

Pyne, T., & Birkinshaw, M. 1993, *ApJ*, 415, 459

Rees, M. J., & Sciama, D. W. 1968, *Nature*, 217, 511

Reese, E. D., Carlstrom, J. E., Joy, M., Mohr, J. J., Grego, L., & Holzapfel, W. L. 2002, *ApJ*, 581, 53

Rephaeli, Y. 1995a, *ARA&A*, 33, 541

———. 1995b, *ApJ*, 445, 33

Rephaeli, Y., & Lahav, O. 1991, *ApJ*, 372, 21

Romer, A. K., et al. 2001, *BAAS*, 199, 1420

Smail, I., Ellis, R. S., Dressler, A., Couch, W. J., Oemler, A., Sharples, R. M., & Butcher, H. 1997, *ApJ*, 479, 70

Spergel, D. N., et al. 2003, *ApJ*, submitted (astro-ph/0302209)

Springel, V., White, M., & Hernquist, L. 2000, *ApJ*, 549, 681 (erratum: 562, 1086)

Sunyaev, R. A., & Zel'dovich, Ya. B. 1972, *Comments Astrophys. Space Phys.*, 4, 173

Trauber, J. 2001, in *IAU Symp. 204: The Extragalactic Infrared Background and its Cosmological Implications*, ed. M. Hauser & M. Harwit (ASP: San Francisco), 40

Worrall, D. M., & Birkinshaw, M. 2003, *MNRAS*, in press (astro-ph/0301123)

M. Birkinshaw

Wright, E. L., Bennett, C. L., Gorski, K., Hinshaw, G., & Smoot, G. F. 1996, ApJ, 464, L21
Zaroubi, S., Squires, G., de Gasperis, G., Evrard, A. E., Hoffman, Y., & Silk, J. 2001, ApJ, 561, 600